

P. DUDEK\*, A. CIAŚ\*

## MICROSTRUCTURE AND MECHANICAL PROPERTIES OF Fe-2.2Mn-1.5Cr-0.2Mo-0.3C STEEL SINTERED AT 1120°C AND 1250°C

## MIKROSTRUKTURA I WŁASNOŚCI MECHANICZNE STALI Fe-2.2Mn-1.5Cr-0.2Mo-0.3C SPIEKANEJ W TEMPERATURACH 1120°C AND 1250°C

In an attempt to study the sinterability of a potential high-strength ferrous alloy Fe-2.2Mn-1.5Cr-0.2Mo-0.3C (AGH2.2-1.5), compacts, based on Höganäs Astaloy Cr-L (Fe-1.5Cr-0.2Mo) water atomised pre-alloyed iron powder, were prepared. Low-carbon ferro-manganese of weight % composition 77Mn-1.3C-0.2O-balance Fe and CU-F graphite were admixed. The samples were sintered at 1120 and 1250°C in a laboratory tube furnaces in nitrogen or 95% nitrogen 5% hydrogen atmospheres with dew points better than  $-70^{\circ}\text{C}$  and cooled at cooling rate  $10\text{Kmin}^{-1}$ . Generally resultant microstructures were homogeneous and consisted of bainite and martensite; they were characterised by the absence of oxide networks. Sintered densities were in the range of  $6.8\text{--}7.0\text{ g/cm}^3$ . Mechanical properties were measured in the as-sintered condition, giving good combination of strength and ductility. Mean fracture strengths of the specimens were 730 MPa in tension and 1170 MPa in bending. The fracture data were analysed using Weibull statistics. This method is often used when evaluating the mechanical properties of “flaw-sensitive”, primarily sintered, materials. By using the Weibull probabilistic relations the resulting variability in the data can be quantified. Weibull moduli,  $m$ , were generally in the range 8–13 for tensile strength and 11–15 for transverse rupture strength.

**Keywords:** sintered steels, sinterhardening, tensile strengths; transverse rupture strength, quasi-brittle fracture, fracture probability, Weibull analysis

W celu zbadania procesu spiekania potencjalnie wysokowytrzymałego stopu żelaza wykonano wypraski, których podstawowym składnikiem był rozpylany, stopowy proszek żelaza Höganäs Astaloy Cr-L (Fe-1.5Cr-0.2Mo). Do proszku tego domieszano proszek niskowęglowego żelazomanganu o składzie 77Mn-1.3C-0.2O (% masowe) – reszta Fe oraz proszek grafitu gatunku C-UF. Wypraski spiekano w temperaturze 1120°C i 1250°C, w laboratoryjnym piecu rurowym, w atmosferze azotu oraz w atmosferze złożonej w 95% z azotu i w 5% z wodoru, o punkcie rosy poniżej  $-70^{\circ}\text{C}$ , po czym próbki chłodzono z prędkością  $10\text{Kmin}^{-1}$ . Badane materiały charakteryzowały się jednorodną mikrostrukturą, składającą się z bainitu i martenzytu oraz cechowały się brakiem siatki tlenków. Własności mechaniczne stopu badano bezpośrednio po spiekaniu. Stop ten ulegał przemianom w strukturę bainityczno-martenzytyczną o dobrej kombinacji wytrzymałości i ciągliwości. Próbki po spiekaniu charakteryzowały się gęstościami od  $6,8\text{ g/cm}^3$  do  $7,0\text{ g/cm}^3$ . Posiadały one średnią wytrzymałości na rozciąganie 730 MPa oraz wytrzymałość na zginanie 1170 MPa. Wyniki badań wytrzymałościowych poddano analizie przy użyciu statystyki Weibulla. Metoda ta jest często stosowana, gdy ocenia się własności wytrzymałościowe materiałów czułych na obecność wad – głównie materiałów spiekanych. Użycie probabilistycznych zależności Weibulla umożliwiło ilościowy opis zmienności uzyskanych wyników badań. Moduły Weibulla,  $m$ , obliczone na podstawie wyników badań wytrzymałości próbek uzyskanych w statycznej próbie rozciągania, mieściły się w przedziale od 8 do 13 oraz od 11 do 15 – w przypadku wyników uzyskanych w oparciu o badanie wytrzymałości na zginanie trójpunktowe.

### 1. Introduction

Chromium and manganese base steels are being evaluated to replace many of nickel-containing systems, due to the relatively low cost of chromium (Cr - \$4500 USD/ton; Ni - \$26000 USD/ton; Mo - \$77000 USD/ton [1]). Particular attention is devoted to complex

Fe-Mn-Cr-C alloys, since they contain inexpensive alloying additions and offer some prospects of commercial utility. Current developments towards high performance PM ferrous structural parts include alloy modifications involving chromium and molybdenum, as evidenced by Höganäs Astaloy CrL powder with 1.5%Cr. Mn contents in some of Stackpole's alloys approach 1% [2]. In our

\* AGH UNIVERSITY OF SCIENCE AND TECHNOLOGY, 30-059 KRAKÓW, 30 MICKIEWICZA AV., POLAND

laboratories alloys containing 1-3% Mn and 1.5-3%Cr have been reproducibly PM processed without the formation of deleterious oxide networks [3-5]. Although tensile strengths can approach 900 MPa with 2% ductility, these alloys compositions and heat treatments remain to be optimised.

This paper deals with the effects of the sintering temperature and atmosphere on microstructure and mechanical properties of Fe-2.2Mn-1.5Cr-0.2Mo-0.3C (AGH2.2-1.5) alloy. The sinterhardening response (hardening during the cooling cycle after sintering) of this PM steels at low cooling rate ( $10\text{Kmin}^{-1}$ ) is investigated. A continuous cooling diagram was created for the alloy of composition now studied, and is reproduced as Fig. 1. It shows that AGH2.2-1.5 steel has good sinterhardening characteristics.

Cias and Mitchell [6,7] have reported on laboratory sintering, at temperatures as low as  $1120^\circ\text{C}$ , of 2-4% manganese steels in dry, hydrogen-rich atmospheres to yield predominantly pearlitic microstructures devoid of oxide networks. This is a significant finding, since numerous previous similar attempts were thwarted by this problem and did not result in industrial exploitation. The majority of the experiments were conducted on 3 Mn-0.6%C alloys and for these  $R_{0.2}$  was in the range 275-500 MPa, tensile strength, (TS), 300-600 MPa, (apparent) transverse rupture strength, (TRS): 640-1260 MPa and plastic strains were up to 7%. When careful control of processing was maintained, reproducibility of mechanical properties was achieved, with the 2-parameters Weibull modulus,  $m$ , attaining a value of 17 [6].

In order to further improve the mechanical properties of PM steel, one or both of the alloying elements Cr and Mn may be added, as already accomplished by Stackpole [2] on an industrial scale. In the current work several approaches are being employed, including the use of already pre-alloyed powders, comprising the newly-introduced Ni-free Astalloy Cr-L, and of ferro-manganese. The processing philosophy involved adding graphite and ferro-manganese fines to standard industrial iron powder grades. The aim is to understand the sintering process of Fe-Mn-Cr-Mo-C steel: in particular the effects of sintering atmosphere on the formation and dissociation of manganese oxide, and sintering temperature on the operating mechanisms. It is postulated that such understanding is beneficial to the development of new compositions of powders and of PM alloy compositions and of their robust processing routes for the manufacture of medium- to-high duty automotive engine components with mechanical properties matching those of wrought steels. On an industrial scale, some Stackpole alloys are already in this category.

An additional advantage of such Fe-Mn-Cr-Mo-C materials is that they do not contain expensive copper and nickel. Copper in steel presents recycling problems and nickel is recognised as allergenic and carcinogenic, which therefore attracts increasingly stringent legislation, e.g. ref. [8].

Some elements used for alloy strengthening in traditional cast and wrought steels, such as Cr and Mn, have been avoided in PM due to their affinity to oxygen and difficulty of reducing their oxides in the process [6,7]. However both Mn and Cr are more effective ferrite strengthening elements than for example Ni and thus are obvious candidates for improved PM alloys providing the sintering process can be sufficiently modified. Mn and Cr tend to form stable oxides and there is no prospect of reducing these at low temperatures in wet, oxygen containing atmosphere. Ellingham-Richardson diagram is a useful tool to predict oxide stability for different temperatures and oxygen pressures. From E-R diagrams it can be seen, that at  $-40^\circ\text{C}$  dew point and for the hydrogen atmosphere the redox line is crossed at  $1250^\circ\text{C}$  for Mn and in excess of  $1000^\circ\text{C}$  for Cr [6,7], although when they are in an alloy form the situation is somewhat more favourable. Therefore oxidation and reduction phenomena at higher temperatures, including the local dew point of the microatmosphere immediately surrounding the compacts, need to be considered. It should be added that this includes manganese vapour and its oxidation and condensation.

In the development of high-strength structural Fe-Cr-Mo-C PM steels with tensile strength  $>500\text{MPa}$ , it is advisable to assess alloys which have sufficient hardenability to avoid the high-temperature pre-eutectoid ferrite reaction on furnace cooling with cooling rate  $\sim 5 - 20\text{Kmin}^{-1}$ , when quenching facilities are not available. Work at AGH has concentrated on using addition of manganese to water atomised pre-alloyed powders for this purpose, and present investigation was intended to determine the optimum amounts of manganese to give a high-strength bainitic structure over a wide range of cooling rates.

A considerable amount of sintering takes place during the heating part of the sintering cycle especially in the case of alloys containing Mo which tend to raise the alpha-gamma transformation temperature. This can lead to the formation of oxide veins within the material, even when using  $\text{H}_2\text{-}25\%\text{N}_2$  sintering furnace atmosphere at dew points as low as  $-70^\circ\text{C}$ . Even the addition of carbon in graphite form does not fully overcome the problem, as significant diffusion of carbon does not seem to occur below  $800^\circ\text{C}$ . It has been noted in the laboratory that a 1% addition of fine elemental Mn has greatly reduced the formation/retention of oxide veins. This is probably due

to the formation of Mn vapour at  $\sim 700^\circ\text{C}$  [6,7], which reacts with the particles and rises the alpha-gamma transformation at these surfaces, thus delaying formation of closed porosity until a sufficiently high temperature has been reached for reduction of chromium oxides. The form in which alloying elements are to be added is probably the most difficult problem. For instance fine ( $\sim 5\mu\text{m}$ ) master alloy, 25Mn-23Cr-22Mo-22Fe-7C-0.10 (MCM), 25.5Mn-23V-25.5Mo-20Fe-5C-0.60 (MVM), 40Mn-20Mo-32Fe-7C-0.30 (MM), additions have been attempted [6]. However, despite initially promising properties when 2-4 wt. % of master alloy was added, this prospective processing route was abandoned due to excessive die wear caused by the grinding action of the alloy carbides (content between 50 and 90% of the master alloy).

Conveyor belt furnaces widely applied in the industry have their limitation in the maximum operating temperature of the high-temperature zone (practicable at 1120 to 1150 $^\circ\text{C}$ ). The recent developments in PM low-alloy structural steels require higher temperature. Sintering a chromium-alloyed material at 1180–1250 $^\circ\text{C}$  gives much better mechanical properties than sintering at 1120 $^\circ\text{C}$ . The improved process conditions cannot be reached economically by using conveyor belt furnace. High-temperature furnaces operating up to 1280 $^\circ\text{C}$  and equipped with sinter-hardening zone are fairly complex and expensive.

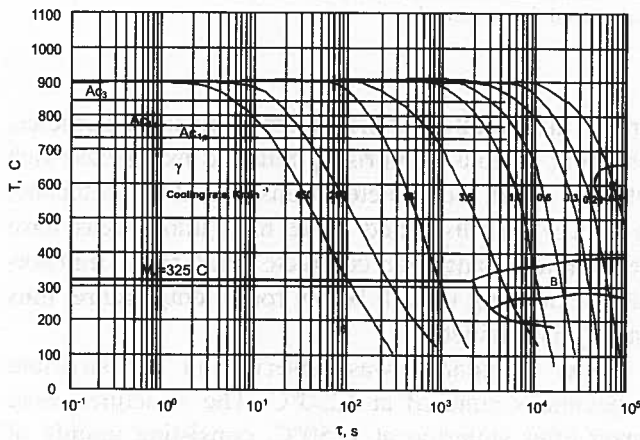


Fig. 1. Continuous cooling transformation diagram for AGH2.2-1.5 steel and several superimposed cooling curves demonstrating the final microstructure; cooling rates taken at 500 $^\circ\text{C}$

## 2. Experimental procedure

For this study, a mix composition based on Höganäs Astaloy CrL prealloyed powder was prepared. Additions were of manganese and carbon; 0.3% of carbon

was introduced as fine Höganäs CU-F fine graphite and 3% of manganese as  $< \mu\text{m}$  Elkem low carbon ferro-manganese powder. The Elkem powder was a by-product, “fines”, from welding electrode production, of composition 77Mn-1.3C-0.20-0.02N-balance Fe.

The choice of nominal alloy final composition AGH2.2-1.5 was influenced by, actual experimentally determined CCT diagrams (Fig. 1) and computer-generated, multi-component phase diagrams. In particular the influences of sintering atmosphere on densification, microstructure and microcompositions were to be investigated.

Mixing and die compaction (typically at 600 MPa), to give green densities in the range 6.8-7.0 g/cm<sup>3</sup>, were followed by sintering in a horizontal laboratory furnace in a nitrogen or nitrogen-rich (N<sub>2</sub>-5% H<sub>2</sub>) atmosphere at 1120 and 1250 $^\circ\text{C}$ . Inlet dew points, in the range -60 to -70 $^\circ\text{C}$  (15 ppm moisture) and gas flow rates were carefully controlled. To produce a Mn-rich micro-atmosphere (“microclimate”, self-gettering effect), the specimens were sintered in a semi-closed stainless steel container with a labyrinth seal. Compacts were heated to the sintering temperature, at a rate of 75Kmin<sup>-1</sup>, and held at 1120 or 1250 $^\circ\text{C}$  for 60 minutes. The convective cooling rate, determined in the temperature range of 1100-500 $^\circ\text{C}$ , was approximately 10Kmin<sup>-1</sup>. The furnace heat resisting Kanthal APM tube included a water-jacketed convective cooling zone.

We made a special effort to obtain the maximum amount of information on the bainitic-martensitic structures encountered. Conventional metallographic examination techniques were used. The tensile bars were sectioned, polished, and prepared for metallographic analysis (etched with 3% nital). These were examined metallographically, including estimates of the volume percentage of these structures, while the percent of retained austenite was determined by an x-ray analysis method. The latter was based on a statistical computer treatment of the data which allows the elimination of detrimental effects of extinction microabsorption.

All mechanical properties were measured using as-pressed ISO 2740 “dog-bone” tensile specimens. Tensile and transverse rupture specimens were tested on mechanical and servo-hydraulic industrial machines at extension rates of  $\sim 0.5\text{mm/min}$ . Young’s modulus and fracture strains were recorded.

## 3. Results

The densities of Fe-Mn-C compacts generally gained 0.1 g/cm<sup>3</sup> on sintering, as shown in Table 1, with specimens sintered at 1250 $^\circ\text{C}$  in N<sub>2</sub>-5%H<sub>2</sub> reaching  $\sim$

7.0 g/cm<sup>3</sup>, 0.2 g/cm<sup>3</sup> larger. Carbon content in the start-

TABLE 1  
Densities of AGH2.2-1.5 (nominal final composition) specimens before and after sintering and final carbon contents

Sintering	Density, g/cm <sup>3</sup>		Carbon content, wt. %
	green	sintered	Sintered
1120°C, N <sub>2</sub>	6.8 ± 0.02	6.9 ± 0.02	0.365
1120°C, N <sub>2</sub> -5%H <sub>2</sub>	6.8 ± 0.04	6.9 ± 0.03	0.363
1250°C, N <sub>2</sub>	6.8 ± 0.08	6.9 ± 0.03	0.3
1250°C, N <sub>2</sub> -5%H <sub>2</sub>	6.8 ± 0.04	7.0 ± 0.05	0.296

$\sigma_n$  - population standard deviation measured for 30 samples

ing powder mixes was 0.4% and after sintering it varied

from 0.296 to 0.365%, Table 1. Carbon losses can be directly related to hydrogen/nitrogen ratio in the sintering atmosphere and to the sintering temperature.

Specimens were tested in tension or simple 3 point bending. The values of hardness (HV<sub>30</sub>), Young's modulus, ultimate tensile strength (UTS) and failure strain and also of TRS (uncorrected) were determined for at least 15 specimens of each batch. The results were averaged and are represented in Table 2.

TABLE 2  
Mechanical properties data for as-sintered specimens AGH2.2-1.5

Sintering	Young's modulus	UTS	Tensile strains to failure (elastic + plastic)	TRS (uncorrected)	Apparent hardness
	GPa	MPa	%	MPa	HV <sub>30</sub>
1120°C, N <sub>2</sub>	130 ± 0.5	630 ± 36	2.5 ± 0.3	1020 ± 65	250 ± 45
1120°C, N <sub>2</sub> -5%H <sub>2</sub>	131 ± 0.8	655 ± 40	2.5 ± 0.2	950 ± 50	260 ± 45
1250°C, N <sub>2</sub>	131 ± 0.8	700 ± 37	3 ± 0.3	1160 ± 70	250 ± 30
1250°C, N <sub>2</sub> -5%H <sub>2</sub>	131 ± 1.3	730 ± 31	3 ± 0.2	1160 ± 50	250 ± 50

$\sigma_n$  - population standard deviation measured for 11 samples

A very important feature of all the microstructures was the absence of oxide networks (Fig.1) frequently characteristic of experimental PM manganese steels [6,7]. If dew point control is inadequate, there is an association of oxygen and manganese, and, to a lesser extent, iron. In specimens correctly processed, as in this investigation, oxygen is hardly detectable. All microstructures were predominantly bainitic, after sintering at 1250°C more homogeneous and comprised only some retained austenite.

In specimens sintered at 1120°C microstructures were inhomogeneous: the transformation to martensite was incomplete and the austenite grains were relatively small. With this material, it appears that the increased transformation to martensite with the accelerated cooling occurs predominantly in the manganese rich areas, which remain partly as retained austenite. Observed were complex structures composed of bainite surrounding a large number of small, substantially unaligned austenitic-martensitic areas, which were partially decomposed to carbide and ferrite, resembling troostite. Partic-

ularly in the vicinities of prior ferro-manganese particles, there were regions comprising retained manganese-rich austenite, which incompletely transformed to martensite. Mn is a  $\gamma$  stabiliser and these high alloy areas have a temperature range for complete martensitic transformation extending to well below room temperature; thus austenite is retained.

Some acicularity was observed in the structure of specimens sintered at 1250°C. The structures were coarser after sintering at 1250°C, consisting mainly of bainitic and martensitic regions. The high-manganese regions usually exhibited structures comprising long coarse martensite laths extending across prior austenite grains and relatively coarse, martensitic needles throughout the microstructure. Between these needles there were regions of almost uniformly dispersed fine martensite, possibly not tempered, intermixed with a light etching retained austenite. It is believed that, on cooling, the martensite transformation is suppressed in these regions, such that a mixed martensitic and retained austenitic phases form.

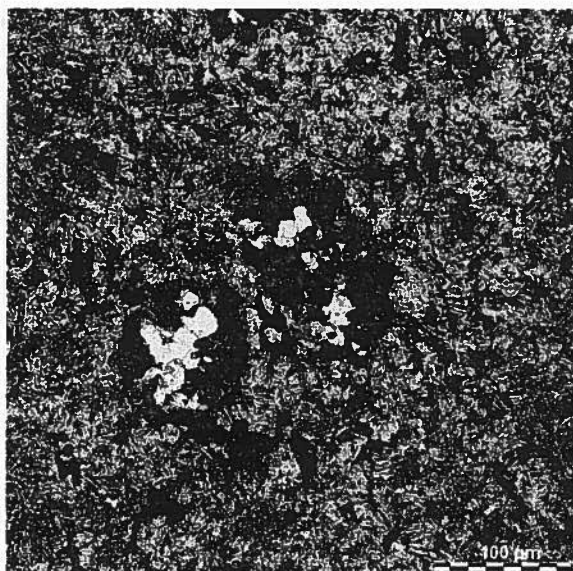


Fig. 2. Microstructure of the specimen sintered in nitrogen at 1120°C

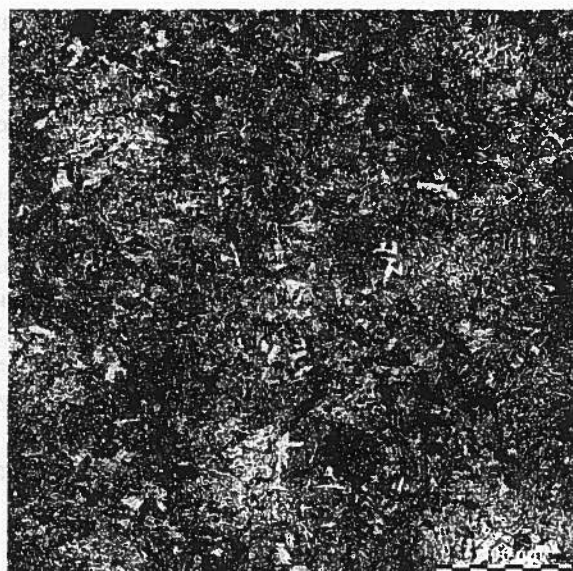


Fig. 3. Microstructure of the specimen sintered in nitrogen at 1250°C

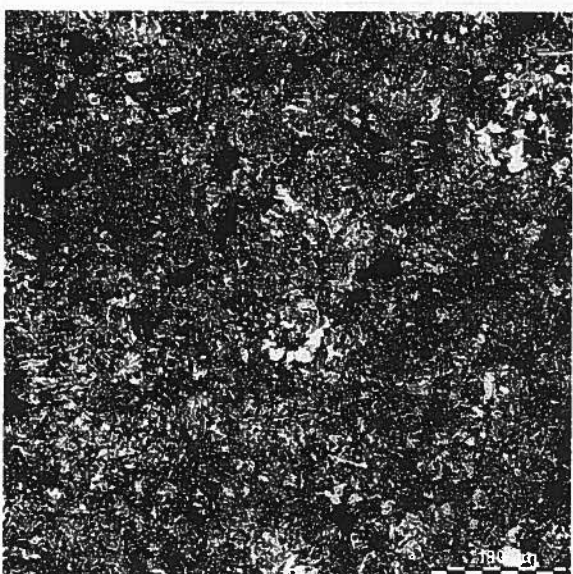


Fig. 4. Microstructure of the specimen sintered in  $N_2$ -5% $H_2$  atmosphere at 1120°C

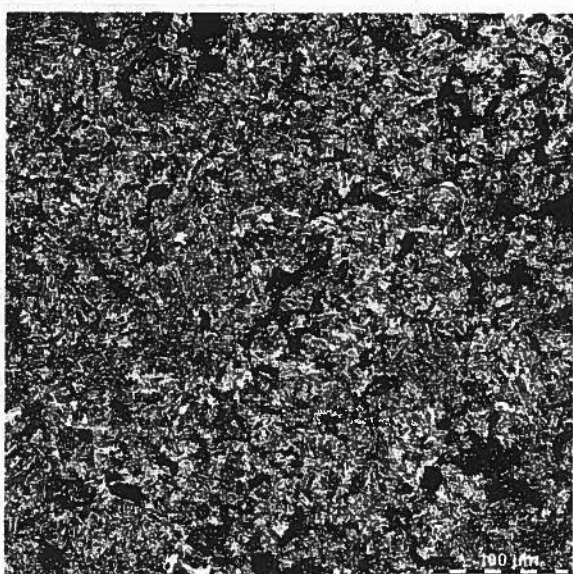


Fig. 5. Microstructure of the specimen sintered in  $N_2$ -5% $H_2$  atmosphere at 1250°C

Since the structures were more or less isotropic, we have generally included them in the bainite class. In some cases, the light-etching particles appear to be austenitic ferromanganese particles partly decomposed to ferrite and carbides. This would account for occasional occurrence of ferritic-bainitic regions containing carbide clusters. An acicular martensite structure can often be detected in the lightly etched areas, clearly in the centre, but less distinctly at the edges of the cross sections of the specimens. In order to establish the nature of these lightly etched particles and thus secure some information on their composition, we carried out sys-

tematic analyses of large number of specimens. X-ray analysis of these specimens generally revealed the presence of residual austenite and carbides ( $M_{23}C_6$ ,  $M_3C$ , and  $M_7C_3$ ). There was, however, no direct correlation between the amount of residual austenite detected by x-ray analysis and the volume of particles, as determined by point counting under microscope. These tests clearly confirmed that some of these particles are two-phase austenite-martensite in spite of their appearance. The residual austenite content in the steel was 6.71-15.8% by x-ray analysis (see Table 3). The highest residual austenite content was found in specimens sintered at 1120°C

in a nitrogen atmosphere. We have been unable to ascertain whether the substitutional-element content of this austenite is different from that of the bulk material, but of its interstitial-elements (carbon and nitrogen) it is raised considerably.

The steels investigated contained dual porosity: both primary and secondary porosity resulting from dissolution of ferro-manganese particles and Mn sublimation, diffusion and condensation. The pores became more rounded in specimens sintered at 1250°C, through greater diffusion of manganese at the higher temperature. There were no significant differences whether sintering was in nitrogen or nitrogen-5% hydrogen, or whether at 1120 or 1250°C; for the latter the pores were rounder, larger and fewer in number.

TABLE 3  
Residual austenite revealed in AGH2.2-1.5 specimens by x-ray analysis

Sintering	Residual austenite content
	%
	green Sintered
1120°C, N <sub>2</sub>	14.2
1120°C, N <sub>2</sub> -5%H <sub>2</sub>	8.03
1250°C, N <sub>2</sub>	15.8
1250°C, N <sub>2</sub> -5%H <sub>2</sub>	6.71

Results of 2-parameter Weibull analysis of UTS and TRS for as-sintered specimens AGH2.2-1.5

TABLE 4

Sintering	2-parameter Weibull analysis								
	UTS			Uncorrected TRS			corrected TRS		
	<i>m</i>	$\sigma_0$ MPa	<i>R</i> <sup>2</sup>	<i>m</i>	$\sigma_0$ MPa	<i>R</i> <sup>2</sup>	<i>m</i>	$\sigma_0$ MPa	<i>R</i> <sup>2</sup>
1120°C, N <sub>2</sub>	9.8 ± 1.6	650	0.94	15.5 ± 2.9	1060	0.97	13.3 ± 2.5	900	0.97
1120°C, N <sub>2</sub> -5%H <sub>2</sub>	8.4 ± 1.4	686	0.95	13 ± 2.5	975	0.94	11.1 ± 2.1	820	0.94
1250°C, N <sub>2</sub>	10.3 ± 1.7	740	0.99	13.6 ± 2.6	1220	0.91	11.8 ± 2.2	1060	0.91
1250°C, N <sub>2</sub> -5%H <sub>2</sub>	12.8 ± 2.1	750	0.92	13.8 ± 2.6	1200	0.97	12 ± 2.3	1040	0.97

$\sigma_n$  – population standard deviation measured for 11 samples

#### 4. Discussion

These materials were optimised to provide high strength. The statistical nature of fracture mechanism requires report of not only a mean strength, but also some parameter describing the distribution of strengths. The fracture data were accordingly analysed using Weibull statistics. Weibull parameters  $\sigma_0$  and *m*, standard error in *m* as well as *R*<sup>2</sup> (*R* – Pearson's correlation coefficient) for the series of at 11 specimens are given in Table 4. Weibull moduli, *m*, quantifying the scatter, were generally in the range 8.4-15.5. The latter value indicates high reproducibility for PM materials. Using stress analyses for plastically deforming bend specimens [6], true maximum tensile stresses were calculated and found higher than tensile strengths. The value of the transverse rupture

strength can exceed that of ultimate tensile strength of the same PM material, identically processed, by a factor up to ~2, although both these parameters relate to the tensile stress causing fracture.

The analysis takes account of the pre-failure plastic strain, which enables conversion of the nominal strengths, UTS and TRS, to true fracture stresses [6,7]. Estimates of maximum stresses in beams of AGH2.2-1.5 alloys undergoing simple elastic-plastic bending are given in Table 4. By taking account of the stress distributions in bend specimens, using Weibull statistics for failure from the same type of flaw, high degree of correspondence was attained between the tensile strength and "normalised" maximum tensile stress in bending. Weibull parameters  $\sigma_0$  and *m*, standard error in *m* as

well as  $R^2$ , are also given in Table 4 (corrected TRS or “normalised” tensile stress in bending).

in nitrogen or nitrogen/hydrogen atmospheres with low dew point and/or use of semi-closed containers to attain the required microatmosphere (“microclimate”). Additionally these problems are reduced at higher sintering temperatures, which further promote homogeneity and pore rounding.

## 5. Conclusions

The results may be summarised as follows:

1. With an alloy of the composition AGH2.2-1.5 it is possible to achieve a minimum UTS of 500MPa and TRS of 900MPa in the as-sintered condition. The data show that by slow cooling from the sintering temperature, in a standard conveyor belt furnace, it is possible to obtain microstructures and mechanical properties that are very similar to those obtained with commercial PM structural steels by conventional quenching and tempering treatments. The combination of sintering and hardening in one step reduces the production costs of low alloy steel parts.
2. It is important to note that while AGH2.2-1.5 PM steel show excellent results after slow cooling, in conditions which can be reached economically by using conveyor belt furnace operated at 1120°C, and not equipped with sinter-hardening zone. Thus this alloy would not be traditionally thought of as a “sinter-hardening” material. It is in fact self-hardening bainitic PM steel with superior mechanical properties.
3. The results do show that mechanical properties can be modified for Mn/Cr sintered steel not only by the presence of martensite, but by control of the bainitic microstructure as a whole. In more inhomogeneous steels sintered at 1120°C martensitic regions with high Mn contents may contain large amounts of retained austenite.

## Acknowledgements

The work described forms part of the research programme supported by a KBN, contract No. 11.11.110.788. The personal thanks of the authors must be especially extended to Prof. dr hab.inż. W. Ratuszek who, with mgr K. Chruściel, did x-ray analysis of the residual austenite content in the steel.

## REFERENCES

- [1] LME Report, London Metal Exchange, April 2008.
- [2] P. K. Jones, P. K. Buckley-Golder K., David H., Lawcock R., Sarafinchan D., Shivanath R., L. Yao: proc. 1998 Powder Metallurgy World Congress, Vol. 3, EPMA, Granada, Spain, 1998, pp.155-166.

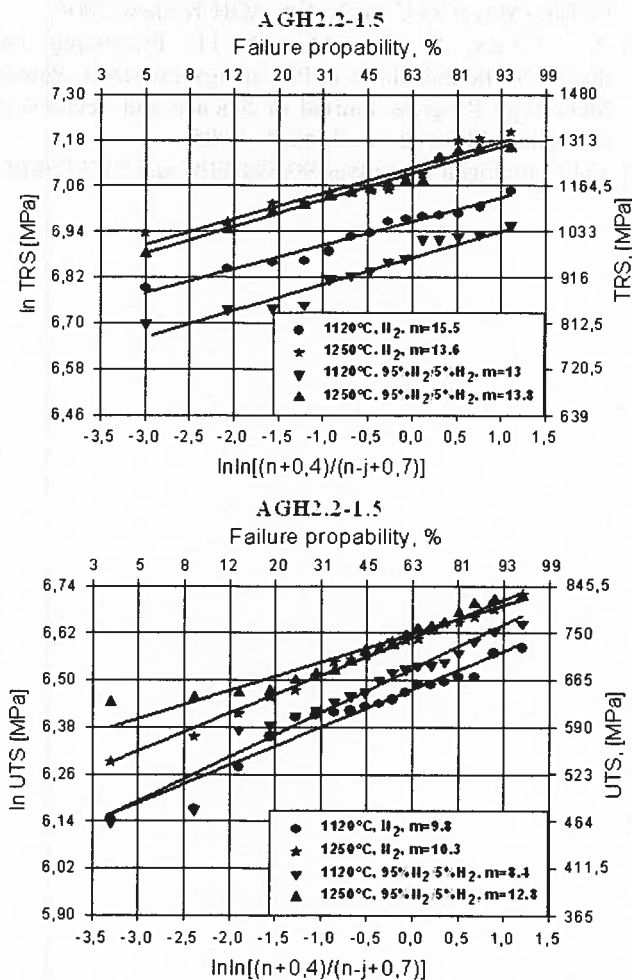


Fig. 6. Comparative Weibull plots of UTS and TRS data of AGH2.2-1.5 steel

Processing in flowing hydrogen-rich atmospheres required dew points dictated by the Ellingham-Richardson diagrams, e.g.  $-55^{\circ}\text{C}$  at 1120 and  $-40^{\circ}\text{C}$  at 1200°C, or attainment of a reducing “microclimate”. This was achieved through the use of semi-closed containers, which ensured the presence of a cloud of manganese vapour. This method was developed and extended using ferro-manganese and carbon as the getter powders or forming part of the green compact [6]. It should further be noted that initially hydrogen was employed as the sintering atmosphere, subsequently nitrogen-hydrogen mixtures and finely dry technical nitrogen. Furnace atmosphere of nitrogen with a dew point of  $-55^{\circ}\text{C}$  proved as successful as sintering in an atmosphere of equally dry hydrogen. Specimens sintered at 1120°C and 1250°C, respectively, possessed similar mechanical properties, irrespective of the  $\text{H}_2\text{-N}_2$  ratio in the furnace atmosphere. It can be stated that the processing drawbacks associated with oxidation of Mn and Cr can be solved by sintering

[3] M. Sułowski, A. Cias, M. Stoytchev, T. Andreev: *Materials Science Forum* **534-536**, 753-756, 2007.

[4] M. Sułowski, A. Cias, H. Frydrych, J. Frydrych, I. Olszewska, R. Goleń, M. Sowa: *Materials Science Forum*, **534-536**, 757-760 2007.

[5] A. Cias, M. Sułowski: *proc. EPMA Int. Pow-*

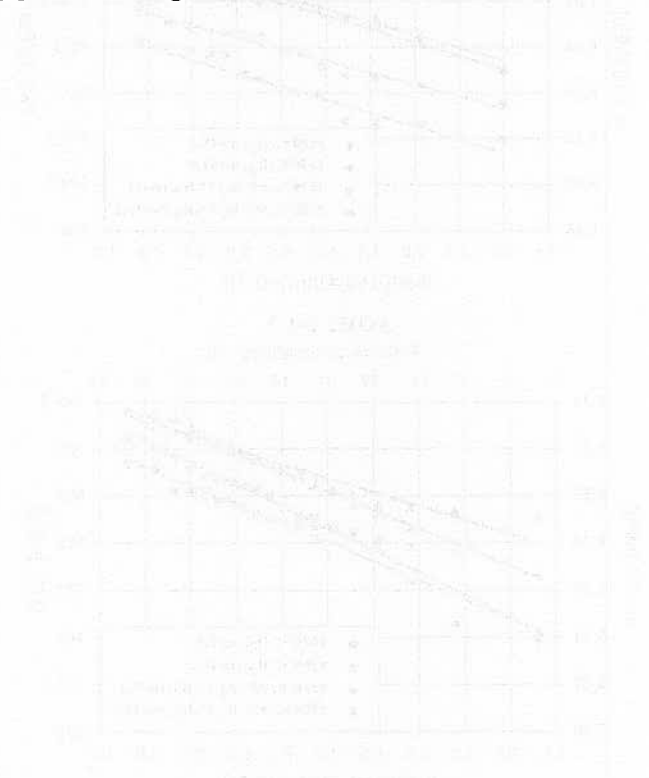
*der Metall. Congress & Exhibit.* : 15-17 October 2007, Toulouse, France, pp. 145-150.

[6] A. Cias: *Development and Properties of Fe-Mn-(Mo)-(Cr)-C steels*. Ed. AGH Krakow 2004.

[7] A. Cias, S. C. Mitchell: *Processing and ductile-brittle transitions in PM manganese steels*, *Powder Metallurgy Progress Journal of Science and Technology of Particle Materials*, **5**, 2, 82-91 2005.

[8] EU Carcinogen Directives 90/394/EEC and 91/322/EEC.

Received: 20 June 2008.



The results of the mechanical tests are presented in the figures. The yield strength and tensile strength of the steels decrease with increasing temperature. The ductile-brittle transition temperature (DBTT) is determined by the intersection of the yield strength and tensile strength curves. The DBTT of the steels is in the range of 400-500°C. The fracture toughness of the steels is also affected by temperature. The fracture toughness of the steels increases with increasing temperature. The fracture toughness of the steels is in the range of 10-20 MPa<sup>1/2</sup>m<sup>1/2</sup>. The fracture toughness of the steels is also affected by the grain size. The fracture toughness of the steels increases with decreasing grain size. The fracture toughness of the steels is in the range of 10-20 MPa<sup>1/2</sup>m<sup>1/2</sup>. The fracture toughness of the steels is also affected by the grain size. The fracture toughness of the steels increases with decreasing grain size. The fracture toughness of the steels is in the range of 10-20 MPa<sup>1/2</sup>m<sup>1/2</sup>.